Commentary

Topological states in photonic systems

Ling Lu, John D. Joannopoulos, Marin Soljačić

Optics played a key role in the discovery of geometric phase. Once again, it joins the journey of exploring topological physics, bringing us bosonic topological states of one-way waveguides, Weyl points and a single surface Dirac cone. At the interfaces of topological photonic materials, the propagation of photons is protected against disorder by the momentum-space topologies in the bulk. Topology equips us with an ability to make perfect photonic devices using imperfect interfaces.

In 1956, Pancharatnam[1] -- a young 22-year old Indian physicist -- showed that, over the course of a cyclic evolution, the polarization vector of light acquires a phase which is only determined by the area of the cycle on the Poincaré sphere. Three years later, the celebrated Aharonov-Bohm phase was discovered[2]. After more than two decades, Berry[3] generalized these two geometric phases into what we now call the "Berry phases. The Berry phase was then demonstrated experimentally in coiled optical fibers[4]. It was immediately realized[5] that the Berry phase is closely connected with the topological interpretation[6] of the integer quantum Hall effect (QHE) discovered in 1980. In particular, the signed integers (Z) in the quantized edge conductance are mathematically equivalent to the bulk Chern numbers of the fiber bundle theory in topology. Another example of the bulk-edge correspondence was shown by Zak[7] that the bulk Berry phase differentiates the Tamm and Shockley states[8], found in the 1930s, at the end of one-dimensional (1D) lattices.

In 1988, Haldane proposed a model[9] suggesting that the QHE can be realized in a band structure with time-reversal-symmetry (*T*) breaking, in which the bands acquire non-zero Chern numbers. This phenomenon is known as the quantum anomalous Hall effect (QAHE). In 2005, Kane and Mele[10] proposed the quantum spin Hall effect (QSHE) by finding that two copies of the Haldane model are also robust, without breaking *T*. This is possible because the crossing points in the band structures are enforced by the Kramers' degeneracy; there is no modal coupling or anti-crossing. This discovery of the QSHE, which is protected by *T*, has led to the broad notion of symmetry-protected topological phases. Since then, countless new topological phases have been theoretically classified and a handful of them experimentally realized, including the 3D topological insulators, topological crystalline insulators and Weyl semimetals. All these topological materials are essentially non-interacting systems of non-trivial band topologies, well described by single-particle band structures. As such, they can also be realized in photonic band dispersions, where photons are the non-interacting bosons.

In this commentary, we briefly summarize the development of topological photonics[11], discuss its uniqueness, and highlight some of the latest progress in the field.

Photons vs. electrons

There is one key distinction between the spin-1 bosons and the spin -1/2 fermions: the *T* operator squares to +1 for bosons, while it squares to -1 for fermions. As a consequence, the topological classifications with respect to *T* are different for the two classes of particles. For example, *T* itself cannot protect a topological phase[11] for bosons. This means *T*-invariant designs in bosonic systems always requires fine-tuning and are intrinsically vulnerable as compared to the fermionic counterparts.

Still, there are many advantages in studying band topologies in photonic systems. First, photons have no Fermi levels --- the energy scales close to which electronic states can be accessed. By contrast, the whole photonic band structure can be probed using photons of different frequencies. Second, photonic lattice structures can be made to design and tuned continuously to create any of the allowed bulk or edge dispersions. The ability to control these structures enables also the study of disorder physics, quasicrystals (see commentary by Krauss&Zilberberg in same issue), and topological defects (see commentary by Lubensky in same issue), which are very difficult in electronic systems. Third, the Maxwell's equations can be solved exactly. Therefore, one can do numerical experiments to support the real experiments. In addition, there is no fundamental length scale in Maxwell's equations: experimentalists can work at any wavelengths (optical, terahertz, microwave) where materials and measurements are most feasible. Lastly, it is easier for photonic research to be translated into applications, as we discuss in the latter section of this commentary.

Another fundamental aspect for electromagnetic fields in the classical regime is the fact that all classical wave fields are intrinsically real-valued (the key feature of topological superconductors as discussed in commentary by Beenakker in same issue). This ensures identical solution at opposite frequency and momenta in the wave equations. Such a built-in "particle-hole" symmetry brings new classes of topological phases with zero-frequency bound states as shown in mechanical systems (see commentary by Huber) as well as in magnetoplasmons[12].

One-way waveguides: QHE of light

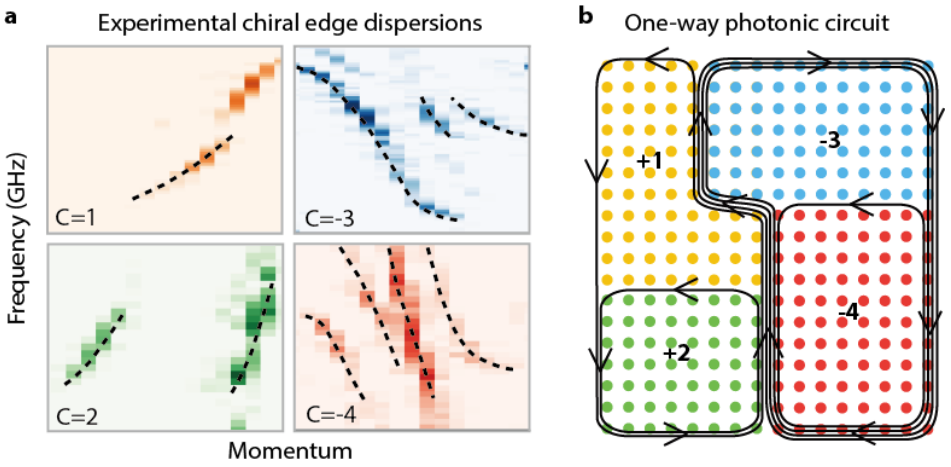

Figure 1 | One-way dispersions and circuit. **a,** Chiral edge dispersions of the one-way waveguides of Chern number 1, 2, -3 and -4, obtained by Fourier-transforming the spatial field profiles of the edge modes. **b,** Illustration of a one-way photonic circuit built by interfacing bulk photonic crystals of different Chern numbers.

In 2005, Haldane and Raghu[13,14] posted an arXiv preprint suggesting that the band structure of the then-elusive QAHE could be realized in a gyroelectric photonic crystal by gapping a pair of Dirac cones under a static magnetic field. Three years later, Wang *et. al* made a realistic design[15] of a gyromagnetic photonic crystal with a Chern number of one. The team also performed the experiments[16], using an array of ferrimagnetic rods inside an electromagnet with a field strength of about a fraction of a Tesla. They made observations at microwave frequencies revealing that the edge mode propagates unidirectionally, and that the transmission is immune to large metallic scatterers. Recently, Skirlo *et. al* found[17] realizations of larger Chern numbers in a similar system by gapping multiple pairs of Dirac cones simultaneously. The authors were able to directly scan the edge mode profiles and Fourier-transform them to observe[18] the chiral dispersions of Chern numbers 1, 2, -3, -4 (Fig. 1a). Such a rich variety of Chern numbers pave the way to integrated one-way photonic circuits, like the one illustrated in Fig. 1b. Unfortunately, since the frequency of gyromagnetic resonance scales with the magnitude of the magnetic field, it is difficult to operate this class of systems towards optical frequencies.

At optical frequencies, T can be broken with time-dependent modulations, also known as in the Floquet systems. Fang *et. al*[19] proposed an array of resonators whose coupling is controlled by dynamic links. Although such a proposal can in principle be realized by modulating the refractive indices, it is technologically challenging for a large-scale lattice. This difficulty is avoided[20] by Rechtsman *et. al* adopting a change of reference frame from the lab to the frame of the photon. They extended the 2D lattice along the third direction into a waveguide array. The waveguides are spirals, so the photons are modulated as they propagate in

the waveguides, allowing an effective breaking of *T* in the photons' reference frame. This experimental demonstration was done at visible wavelengths.

T-invariant designs

Due to the difficulty in breaking *T* at optical frequencies, *T*-invariant 2D topological phases (analogous to the QSHE) with robust counter-propagating helical edge states are highly desirable. However, due to the lack of Kramer's degeneracies, two counter-propagating bosonic edge states will in general couple and backscatter. Luckily, photonic systems have a large amount of freedom for designers. Fine-tuning the system parameters could minimize the modal coupling and achieve near-reflectionless propagation without breaking *T*. In the first example, Hafezi *et. al.*[21] , by assuming the absence of local imperfections, created two copies of the QHE edge states by artificial gauge fields. They connected a 2D array of ring cavities through waveguides with different lengths to mimic the Aharonov-Bohm phase of electrons under a uniform magnetic field (later Liang *et. al.*[22] showed that the waveguides could be simplified to be identical). The team fabricated[23] this system on a silicon-on-insulator chip using standard CMOS technology and observed the edge states at near infrared wavelength. Such a reciprocal system is robust against variations in the resonator frequencies, but it remains vulnerable to local defects[24].

In the second *T*-invariant 2D system, Khanikaev *et. al.*[25] mimicked the QSHE using the two polarization states by matching the permittivity (ε) and permeability (μ) values in metamaterials. Such a symmetry in the constitutive relations guarantees the separation of polarization modes. Polarized edge states flow in both directions and do not scatter into each other as long as the ratio of ε / μ of the whole system is identical, both in the bulk and on the edge. Chen *et. al.*[26] realized this proposal by embedding a metamaterial photonic crystal inside a parallel-plate metallic waveguide. Cheng *et. al.*[27] showed that certain types of reduction of back-reflection can be achieved in a more practical design, relaxing the strict ε-μ requirement.

In the third example, Wu *et. al.*[28] showed theoretically that topological phase transition can take place in the bulk of a 2D photonic crystal invariant under C_6 rotation. Unfortunately, there are no protected edge states, because C_6 symmetry cannot be satisfied on the 1D edge. However, by tuning the edge configuration, the anti-crossing gap between the two counter-propagating edge states can be very small, meaning a diminishing back-reflection.

Berry charges: Weyl points

Connecting equivalent boundaries of a Brillouin zone in 2D gives a toroidal topology. The Chern number of a 2D band can be understood as the number of

Berry monopoles inside the torus, emitting quantized Berry flux through the dispersion band. In the 3D momentum space, the Berry monopole is a Weyl point --- a 3D linear point degeneracy between two bands. Topological charges are robust in the 3D momentum space and can only be annihilated pairwise with the opposite charge: this provides a general way to obtain 3D topological gapped phases. Similar to the edge states of the one-way waveguides, the surface state of a Weyl crystal is also gapless, due to the non-zero Chern numbers in the bulk.

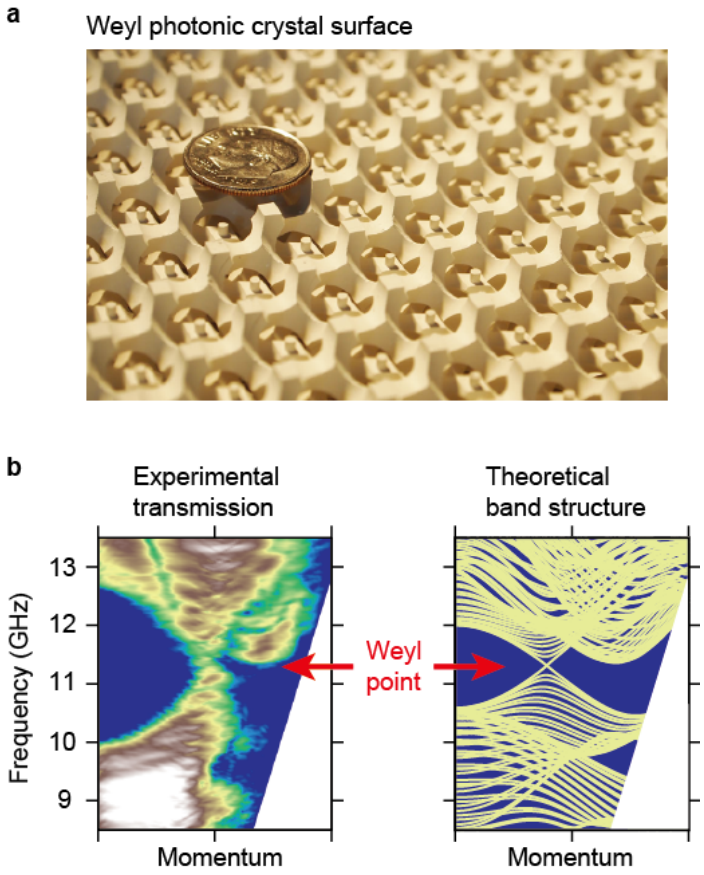

Figure 2 | Weyl points in a gyroid photonic crystal. **a,** The surface of the non-centrosymmetric double-gyroid photonic crystal with a dime on top. **b,** The microwave transmission intensity through the sample, comparing very well to the projected Weyl band structure in theory.

Lu *et. al.*[29] theoretically proposed the existence of Weyl points in a double-gyroid 3D photonic crystal, by either breaking the time or the inversion symmetry. In both cases, they obtained the minimal number of Weyl points that are frequency-isolated in the Brillouin zone with topologically non-trivial surface states. Recently, the team experimentally[30] fabricated such a gyroid crystal by breaking inversion. Microwave transmission measurements revealed the linear bulk dispersion, the signature of the long-sought Weyl quasi-particle originally proposed in 1929.

A gapless surface state similar to that of the Weyl crystal can exist on the surface of a 3D bianisotropic hyperbolic material, as predicted by Gao *et. al.*[31]. In contrast to regular lattices of discrete translations, this bulk bianisotropic medium is invariant under continuous translations. Recently, Silveirinha[32] showed how Chern numbers could be defined in continuous dispersive media, indicating that previously-known one-way plasmonic modes have topological origins.

Disorder-immune surface: a single Dirac cone

In 2D band structures, the topological phase transition takes place when the band structure has Dirac cones: gapping them can form bandgaps that support gapless edge states. In 3D, such a transition is generally a stable phase of Weyl points. When Weyl points annihilate, 3D topological bandgaps can form, supporting gapless surface states.

Lu *et. al.*[33] theoretically identified a 3D photonic crystal supporting two Weyl points (of opposite Chern numbers) stabilized at the boundary of the 3D Brillouin zone, and forming a novel linear four-fold point-degeneracy. Such a generalized 3D Dirac point is protected by the non-symmorphic crystal symmetries of the lattice. The team then broke T to gap the 3D Dirac points while preserving the glide reflection – the non-symmorphic operation that can be preserved on the surface. The resulting magnetic crystal supports a single Dirac cone on its surface protected by the glide reflection--- this result is the first material prediction of a 3D gapped bosonic topological phase, characterized by a Z_2 (binary) topological invariant. It can be regarded as the bosonic analogue of either the 3D topological insulators featuring single surface Dirac cones or the topological crystalline insulators protected by crystal symmetries.

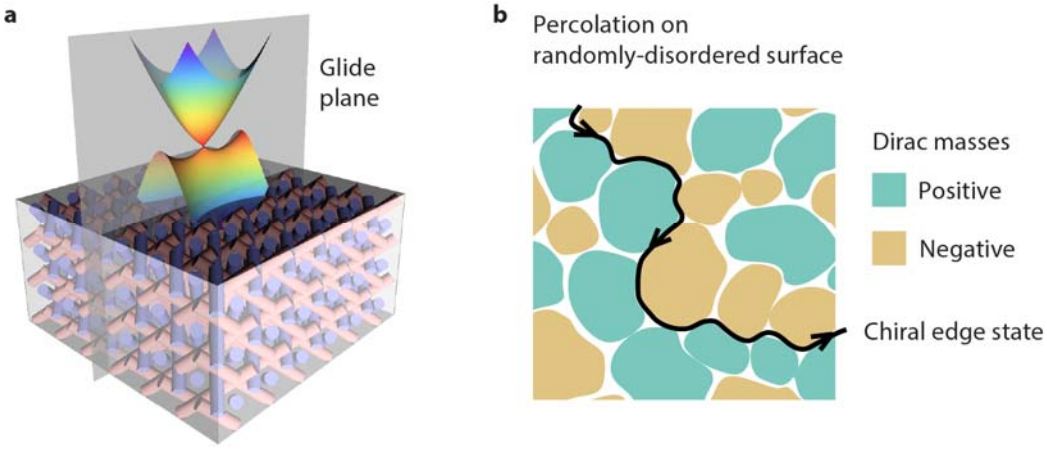

Figure 3 | A single-Dirac-cone surface state immune to random disorder. **a,** Illustration of a 3D magnetic photonic crystal supporting a single Dirac cone on its surface, protected by a glide-reflection plane. **b,** The surface state remains

delocalized under any disorder that, on average, does not break the glide-reflection symmetry.

A single Dirac cone surface state remains gapless under random disorder of arbitrary kind. There always exists an extended state delocalized on the magnetic surface, such as that illustrated in Fig. 3b. Without disorder, the surface photon propagates as a massless Dirac particle in 2D. In a disordered region, the Dirac particle acquires a mass if the glide reflection is locally broken. Depending on the nature of the disorder, this mass term can either be positive or negative. The random distribution of disorder ensures that the masses of opposite signs are equally populated on the surface. At the 1D interface where the mass changes sign, a massless solution has to exist. This turns out to be the same solution of the chiral edge states in one-way waveguides. Consequently, these one-way edges states percolate the whole surface, leading to the absence of Anderson localization.

Potential applications

The quality of traditional optical elements relies on the ability to polish optically smooth surfaces. In nanophotonics, processes like lithography, deposition and etching define the quality of the devices. In both cases, the fabrication capability plays a critical role in achieving state-of-art performance. Today, topology opens up a whole new degree of freedom. The transport of many topological interfacial states is immune to fabrication imperfections; this has been shown in the above examples of one-way waveguides on the 1D edge and of single-Dirac-cone states on the 2D surface. With one-way waveguides, one doesn't need to worry about waveguide bends, coupling efficiencies, or the integration of isolators. The 2D topological surface could potentially be used in surface sensing and florescence counting. In contrast to a regular optical system where the number of states grows rapidly with the system size, the number of modes at Dirac and Weyl points does not scale with the cavity size; this unique feature (among other benefits) might enable single-mode lasers over a larger area or volume. Furthermore, the topological states absent of Anderson localizations may open new opportunities for the slow-light[34] technology that so far has been hindered by the localization of light due to disorder.

The search for topological interfacial states also inspired the reexamination of other robust phenomena in optics. For example, Zhen *et. al.*[35] pointed out that the robust optical bound states in continuum are, in fact, the vortex cores of the far-field polarization, in which the topological invariant is the winding number of the polarization vector. These topological bound states (quite different from the other topological phenomena described in this commentary) can be used to generate vector beams whose beam angles can be continuously steered.

Future directions

In 2D, there is an urgent need to achieve one-way waveguides at optical wavelengths. In 3D, Weyl points and the single-Dirac-cone surface states indicate the opportunity of various 3D topological phases that could be protected by spatial symmetries. There are 230 space groups and 1651 magnetic groups. By controlling the photon lifetime, one could explore the opportunities in non-Hermitian systems[36]. Besides, the experience with photonic topological states can be readily applied to other bosonic particles, such as phonons (see commentary by Huber in same issue), magnons, excitons, polaritons, plasmons[12] and cold atoms (see commentary by Zoller in same issue). Last but not the least, interactive topological phases of light can potentially be achieved by photon interactions mediated by highly non-linear elements, shedding light on many-body physics such as the fractional quantum Hall effect[37].

Ling Lu was and John D. Joannopoulos and Marin Soljačić are in the Department of Physics, Massachusetts Institute of Technology, Cambridge 02139, USA. Ling Lu's present address is Institute of Physics, Chinese Academy of Sciences, Beijing 100190, China

References

1. Pancharatnam, S. *Proc. Indiana Acad. Sci. A* **44,** 247–262 (1956).
2. Aharonov, Y., Bohm, D. *Phys. Rev.* **115,** 485 (1959).
3. Berry, M. V. *Proc. R. Soc. A* **392,** 45 (1984).
4. Tomita, A., Chiao, R. Y. *Phys. Rev. Lett.* **57,** 937 (1986).
5. Simon, B. *Phys. Rev. Lett.* **51,** 2167 (1983).
6. Thouless, D. J. , Kohmoto, M., Nightingale, M. P., den Nijs, M. *Phys. Rev. Lett.* **49,** 405 (1982).
7. Zak, J. *Phys. Rev. Lett.* **62,** 2747 (1989).
8. Shockley, W. *Phys. Rev.* **56,** 317 (1939).
9. Haldane, F.D.M. *Phys. Rev. Lett.* **61,** 2015 (1988).
10. Kane, C.L., Mele, E. J. *Phys. Rev. Lett.* **95,** 226801 (2005).
11. Lu, L., Joannopoulos, J. D., Soljačić, M. *Nature Photon.* **8,** 821-829 (2014).
12. Jin, D., *et al.* Preprint at http://arxiv.org/abs/1602.00553 (2016).
13. Haldane, F. D. M., Raghu S. *Phys. Rev. Lett.* **100,** 013904 (2008).
14. Raghu, S., Haldane, F. D. M. *Phys. Rev. A* **78,** 033834 (2008).
15. Wang, Z., Chong, Y.D., Joannopoulos, J.D., Soljacic, M. *Phys. Rev. Lett.* **100,** 013905 (2008).
16. Wang, Z., Chong, Y.D., Joannopoulos, J.D., Soljacic, M. *Nature* **461,** 772 (2009).
17. Skirlo, S., Lu, L., Soljačić, M. *Phys. Rev. Lett.* **113,** 113904 (2014)

18. Skirlo, S.A., *et al. Phys. Rev. Lett.* **115**, 253901 (2015)
19. Fang, K., Yu, Z., Fan, S. *Nature Photon.* **6,** 782–787 (2012).
20. Rechtsman, M. C. et al. *Nature* **496,** 196–200 (2013).
21. Hafezi, M., Demler, E. A., Lukin, M. D., Taylor, J. M. *Nature Phys.* **7,** 907–912 (2011).
22. Liang, G. Q., Chong, Y. D. *Phys, Rev. Lett.* **110,** 203904 (2013).
23. Hafezi, M., Mittal, S., Fan, J., Migdall, A., Taylor, J. M. *Nature Photon.* **7,** 1001–1005 (2013).
24. Gao, F. *et al.* Preprint at http://arxiv.org/abs/1504.07809 (2015).
25. Khanikaev, A. B. *et al. Nature Mater.* **12,** 233–239 (2013).
26. Chen, W. *et al. Nature Commun.* **5**, 5782 (2014).
27. Cheng, X. *Nature Mater.* **15,** 542–548 (2016).
28. Wu, L. H., Hu, X. *Phys. Rev. Lett.* **114,** 223901 (2015).
29. Lu, L., Fu, L., Joannopoulos, J. D. & Soljačić, M. *Nature Photon.* **7,** 294–299 (2013).
30. Lu, L. *et al*. *Science*, **349,** 622-624 (2015).
31. Gao, W. *et al. Phys. Rev. Lett.* **114,** 037402 (2015).
32. Silveirinha, M.G., *Phys. Rev. B* **92,** 125153 (2015).
33. Lu, L. *et al. Nature Phys.* **12,** 337–340 (2016).
34. Yang, Y, et al. Appl. Phys. Lett. **102**, 231113 (2013).
35. Zhen, B., Hsu C.W., Lu, L., Stone A.D., Soljačić, M. *Phys. Rev. Lett.* **113,** 257401 (2014).
36. Zeuner, J. M. *et al. Phys. Rev. Lett.* **115,** 040402 (2015).
37. Umucalılar, R. O., Carusotto. I. *Phys. Rev. Lett.* **108,** 206809 (2012).

Acknowledgements

We thank P. Rebusco for critical reading and editing of the manuscript. J.D.J. was supported in part by the U.S. Army Research Office through the Institute for Soldier Nanotechnologies under contract W911NF-13-D-0001. L.L. was supported in part by the Materials Research Science and Engineering Center Program of the NSF under award DMR-1419807. M.S. was supported in part by the MIT Solid-State Solar-Thermal Energy Conversion Center and Energy Frontier Research Center of DOE under grant DE-SC0001299.